Application of recyclable CRISPR/Cas9 tools for targeted genome editing in the postharvest pathogenic fungi *Penicillium digitatum* and *Penicillium expansum*

Sandra Garrigues*, Paloma Manzanares and Jose F. Marcos

Food Biotechnology Department, Instituto de Agroquímica y Tecnología de Alimentos (IATA), Consejo Superior de Investigaciones Científicas (CSIC), Catedrático Agustín Escardino Benlloch 7, 46980 Paterna, Valencia, Spain.

*Corresponding author: Sandra Garrigues sgarrigues@iata.csic.es

Abstract

Penicillium digitatum and *Penicillium expansum* are plant pathogenic fungi that cause the green and blue mold diseases, respectively, leading to serious postharvest economic losses worldwide. Moreover, *P. expansum* can produce mycotoxins, which are hazardous compounds to human and animal health. The development of tools that allow multiple and precise genetic manipulation of these species is crucial for the functional characterization of their genes. In this sense, CRISPR/Cas9 represents an excellent opportunity for genome editing due to its efficiency, accuracy and versatility. In this study, we developed protoplast generation and transformation protocols and applied them to implement the CRISPR/Cas9 technology in both species for the first time. For this, we used a self-replicative, recyclable AMA1-based plasmid which allows unlimited number of genomic modifications without the limitation of integrative selection markers. As test case, we successfully targeted the *wetA* gene, which encodes a regulator of conidiophore development. Finally, CRISPR/Cas9-derived Δ*wetA* strains were analyzed. Mutants showed reduced axenic growth, differential pathogenicity and altered conidiogenesis and germination. Additionally, *P. digitatum* and *P. expansum* Δ*wetA* mutants showed distinct sensitivity to fungal antifungal proteins (AFPs), which are small, cationic, cysteine-rich proteins that have become interesting antifungals to be applied in agriculture, medicine and in the food industry. With this work, we demonstrate the feasibility of the CRISPR/Cas9 system, expanding the repertoire of genetic engineering tools available for these two important postharvest pathogens and open up the possibility to adapt them to other economically relevant phytopathogenic fungi, for which toolkits for genetic modifications are often limited.

Keywords

Genome editing, CRISPR/Cas9, *Penicillium digitatum, Penicillium expansum, wetA,* AMA1-based plasmid.

36 **1. Introduction**

37 Fungal plant pathogens cause serious losses and damages to agricultural products worldwide.
38 Postharvest pathogenic fungi can blemish, disfigure and cause fruits rot, significantly reducing
39 their market value (Snowdon 1988). Additionally, infected products pose a potential risk since
40 some decay fungi produce mycotoxins that are hazardous to human and animal health (Liu et
41 al. 2020).

42 *Penicillium digitatum* and *Penicillium expansum* are fungal phytopathogens that cause the green
43 and blue mold diseases in harvested fruits, respectively (Ballester et al. 2014; Marcet-Houben et
44 al. 2012). Although these two species are closely related, they differ in their host specificity.
45 Whereas *P. digitatum* is restricted to citrus fruits (Marcet-Houben et al. 2012), *P. expansum*
46 infects a wide range of pome and stone fruits, including apples, pears, and to a lesser extent
47 peaches and grape berries, among others (Julca et al. 2016). Despite the application of
48 fungicides and alternative strategies, the green and blue mold diseases continue to place high
49 infection pressures on stored fruits worldwide (Vilanova et al. 2012). Besides their negative
50 impact for the fruit industry, *P. expansum* additionally produces patulin and citrinin, two toxic
51 mycotoxins that can contaminate infected fruits and their derived products (Ballester et al. 2014;
52 Morales et al. 2007). Due to the industrial and social relevance of these two postharvest
53 pathogens, many efforts have focused on the characterization of the genetic and molecular
54 mechanisms involved in pathogenicity, virulence, fungicide resistance, and mycotoxin
55 production (Ballester et al. 2019; Costa et al. 2019; Chen et al. 2018; de Ramón-Carbonell and
56 Sánchez-Torres 2017; Gandía et al. 2019a; Gandía et al. 2019b; Gandía et al. 2014; Garrigues
57 et al. 2020; Harries et al. 2015; Li et al. 2020; Zhang et al. 2013). In this sense, precise and
58 versatile methods for genetic manipulation of these fungi are needed.

59 CRISPR/Cas9 (Clustered Regularly Interspaced Short Palindromic Repeats/CRISPR-
60 associated protein-9 endonuclease) (Jinek et al. 2012) has revolutionized high-throughput

61 functional genomics, and has become a common genome editing system in a variety of
62 organisms, including filamentous fungi (Kun et al. 2019). This technology is based on the ability
63 of Cas9 endonuclease to precisely recognize and cut a specific DNA sequence, generating
64 double strand breaks (DSBs). Its specificity relies on a single RNA sequence (guide RNA,
65 gRNA) which can be designed to target a specific (and complementary) genetic sequence
66 through the interaction with the so called Protospacer Adjacent Motive (PAM). *Streptococcus*
67 *pyogenes* SpCas9 protein is one of the preferred Cas endonucleases to date mainly due to the
68 abundance of its target PAM sequences (5'-NGG-3') within the genomes (Jinek et al. 2012).
69 Once the DNA cutting occurs, DSBs are detected as potentially lethal damage and need to be
70 repaired. In eukaryotic systems like filamentous fungi, two DNA repair mechanisms co-exist: (i)
71 the error-prone non-homologous end-joining (NHEJ) (Davis and Chen 2013), and (ii) the high-
72 fidelity homology-directed repair (HDR), which occurs in the presence of a homologous DNA
73 template, often referred as donor DNA (dDNA) or as rescue template (RT), via homologous
74 recombination (HR) (Wright et al. 2018).

75 The first application of CRISPR/Cas9 in filamentous fungi was in the industrially relevant
76 *Trichoderma reesei* (Liu et al. 2015) and six *Aspergillus* species (Nødvig et al. 2015). Since
77 then, CRISPR/Cas9 has enabled the genetic manipulation of a variety of fungal species,
78 including economically relevant plant pathogenic fungi such as *Pyricularia* (*Magnaporthe*)
79 *oryzae* (Arazoe et al. 2015), *Alternaria alternata* (Wenderoth et al. 2017), *Fusarium*
80 *graminearum* (Gardiner and Kazan 2018), *Botrytis cinerea* (Leisen et al. 2020), or *Claviceps*
81 *purpurea* (Králová et al. 2021).

82 Despite the numerous examples on the application of CRISPR/Cas9 in fungi already in
83 literature, the establishment of the CRISPR/Cas9 system in filamentous fungi is not
84 straightforward, and its efficiency differs depending on the species under study. Although the
85 CRISPR system has been widely applied in many Aspergilli (Son and Park 2021), its

implementation in *Penicillium* species remains challenging. Currently, very few studies reported the feasibility of application of CRISPR/Cas9 in *Penicillium* species despite the great interest of this genus at the biotechnological and industrial level, those being *Penicillium rubens* (formerly identified as *Penicillium chrysogenum*) (Pohl et al. 2016), *Penicillium subrubescens* (Salazar-Cerezo et al. 2020), *Penicillium oxalicum* (Wang et al. 2021), *Penicillium polonicum* (Valente et al. 2021), and *Penicillium roqueforti* (Seekles et al. 2021).

The alternatives for the application of CRISPR/Cas9 are the delivery of *in vitro* pre-assembled Cas9 ribonucleoproteins; the transient expression of Cas9/gRNA; through self-replicating AMA1-based plasmids or the stable integrative approaches (Wang and Coleman 2019). Self-replicating AMA1-based non-integrative expression systems have the main advantages of the recycling of the system -allowing unlimited number of genomic modifications without the limitation of integrative selection markers-; and the non-integrating *cas9* gene, which minimizes the risk of genotoxicity.

To date, genetic engineering of *P. digitatum* and *P. expansum* has only been achieved through *Agrobacterium tumefaciens*-mediated transformation (ATMT) and homologous recombination protocols (Buron-Moles et al. 2012; Wang and Li 2008). However, ATMT typically results in genome integrations that often require the presence of selection markers for transformant selection, which can be a major limitation for multiple transformation events. In this study, we developed a protoplast-mediated transformation (PMT) method and implemented the CRISPR/Cas9 genome editing technology in both *P. digitatum* and *P. expansum* for the first time. As a test case, we successfully disrupted the *wetA* gene by using a non-integrative, self-replicative, recyclable CRISPR/Cas9 plasmid. This gene has been reported to encode a regulator of conidiophore development in economically relevant filamentous fungi such as several *Fusarium, Aspergillus* and *Penicillium* species (Prade and Timberlake 1994; Son et al. 2014; Tao and Yu 2011; Wu et al. 2018; Wu et al. 2017), including *P. digitatum* (Wang et al.

111 2015) resulting in white-sporulated colonies. However, no information about its role in *P.*
112 *expansum* was previously available. Finally, the effects of the *wetA* disruption on growth,
113 conidia production and germination rates, sensitivity to antifungal compounds, and pathogenicity
114 in both *P. digitatum* and *P. expansum* are reported.

115 **2. Material and methods**

116 **2.1. Strains, media and growth conditions**

117 The fungal strains *P. digitatum* CECT 20796 (isolate PHI26) (Marcet-Houben et al. 2012) and
118 *P. expansum* CECT 20906 (CMP-1) (Ballester et al. 2014) were used as parental strains. These
119 strains and transformants generated in this study were routinely cultured on potato dextrose
120 agar (PDA) plates (Difco-BD Diagnostics) for 5-7 days at 25 ºC. Conidia were subsequently
121 harvested, dispersed in sterile Milli-Q H_2O, and the concentration was adjusted using a
122 hemocytometer. To analyze growth on solid plates, 5 µL of conidia suspension (5×10^4
123 conidia/mL) of parental and mutant strains were deposited in the center of PDA plates, and the
124 growth diameter was measured from 3 to 7 days. Assays were performed in technical triplicates.
125 Finally, vectors generated in this study were propagated in *E. coli* JM109 grown in Luria Bertani
126 (LB) medium supplemented with 25 µg/mL chloramphenicol (Sigma-Aldrich) at 37 °C.

127 **2.2. Generation of DNA constructs**

128 The CRISPR sites for the design of gRNA sequences were identified using the Geneious Prime
129 software version 11.0.4 (https://www.geneious.com/). The 20 bp spacer sequences for the
130 gRNAs (Table 1) with no off-targets and high on-target activity were predicted based on the
131 experimentally validated predictive model by (Doench et al. 2014). All genetic modifications
132 were designed with either *P. digitatum* CECT 20796 or *P. expansum* CECT 20906 genome and
133 annotation (Ballester et al. 2014; Marcet-Houben et al. 2012). The gRNA sequences were

134 synthesized (Integrated DNA technology, IDT) and used to target the *wetA* gene in *P. digitatum*
135 (gene ID: PDIG_73870) and *P. expansum* (gene ID: PEX1_019290).

136 Derivatives of the self-replicative CRISPR/Cas9 plasmid pLM-AMA15.0 (AddGene ID #138944)
137 (Supplementary Fig. S1) to target *wetA* genes in both *P. digitatum* and *P. expansum* were
138 constructed following previous guidelines (Mózsik et al. 2021). The gRNA backbone and the
139 hepatitis delta virus (HDV) ribozyme are supplied on the AMA1-vector pLM-AMA15.0 together
140 with the *lacZ* gene flanked by *Bsa*I restriction sites. The 20 bp spacer sequence defining the
141 CRISPR site was supplied on a separate DNA sequence together with the hammerhead
142 ribozyme (HH), which includes the 6 bp inverted repeat of the 5′-end of the spacer to complete
143 the HH cleavage site. This DNA molecule was generated by PCR using two overlapping primers
144 (Table 1) and subsequently purified (High Pure PCR Cleanup Micro Kit, Sigma-Aldrich). The
145 fragment was then inserted into pLM-AMA15.0 through *Bsa*I restriction sites (*Bsa*I,
146 ThermoFisher scientific) and T4 DNA ligase (Promega) with a vector/insert ratio of 1/100 by
147 Golden gate modular assembly (Engler et al. 2009). Positive bacterial clones were detected with
148 blue/white screening in the presence of 0.1 mM isopropyl β-d-1-thiogalactopyranoside (IPTG)
149 and 50 µg/mL 5-bromo-4-chloro-3-indolyl-β-D-galactopyranoside (Xgal). Finally, correct
150 sequence integrations were verified through PCR reaction (NZYTaq II DNA polymerase,
151 Nzytech) (Table 1) and plasmids were isolated using NZYMiniprep kit (Nzytech).

152 The homology-based RTs were constructed to delete *wetA* genes in both *P. digitatum* and
153 *P. expansum* through HR. All RTs were obtained through fusion PCR amplification using
154 NZYTaq II DNA polymerase (Nzytech) following manufacturer's instructions. First, two PCR
155 fragments were generated by amplifying ≈ 1500 bp upstream and downstream of the
156 *P. digitatum* and *P. expansum wetA* genes. Finally, these two fragments were fused together in
157 a second 'nested' PCR reaction obtaining ≈ 2400 bp RT with approximately 1200 bp homology
158 arms to both upstream and downstream regions of the *wetA* genes. RTs were subsequently

159 purified (High Pure PCR Product Purification Kit, Roche) and co-transformed with the pLM-
160 AMA15.0 plasmid. All the primers used to generate the RTs are listed in Table 1.

161 **2.3. Protoplast generation, fungal transformation and mutant confirmation**

162 All media and solutions for protoplasts generation and transformation are described in
163 Supplementary Table S1. Protoplasts from *P. digitatum* CECT 20796 and *P. expansum* CECT
164 20906 were generated as follows: a final concentration of 4×10^6 and 1×10^6 conidia/mL of
165 *P. digitatum* and *P. expansum* spores, respectively, were inoculated in 2 L plastic Erlenmeyer
166 flasks containing 250 mL of either *P. digitatum* transformation medium (PdTM), or *Aspergillus*
167 transformation medium for *P. expansum* (TM) at 25 ºC and 250 rpm. After 24 or 18 h of growth
168 of *P. digitatum* and *P. expansum*, respectively, the culture was filtered through sterile Miracloth,
169 washed with 0.6 M $MgSO_4$, and dried. The mycelia were then dissolved in PS buffer with a
170 resuspension ratio of 6.5 mL PS/g mycelium and mixed well with the VinoTaste® Pro lysing
171 enzyme (Novozymes) preparation (0.5 g enzyme/g mycelium in 10-15 mL PS). The mix was
172 incubated in a rotary shaker at 30 ºC, 80 rpm, for 2 and 3 h in the case of *P. digitatum* and *P.*
173 *expansum,* respectively. Protoplast suspensions were placed on ice, and filtered through sterile
174 Miracloth paper. Cold SC solution was added to reach 45 mL suspension volume. Protoplasts
175 were centrifuged for 10 min, 1700 × *g,* 4 ºC and washed with 10 mL of solution B. Protoplast
176 suspensions were then centrifuged for 10 min, 750 × *g,* 4 ºC, and finally resuspended in solution
177 B to a final protoplast concentration of $1\text{-}2 \times 10^7$ protoplasts/mL prior to transformation. A
178 schematic representation of the protoplast generation protocol is shown in Fig. 1.

179 For transformation, 200 µL of protoplasts ($1\text{-}2 \times 10^7$ protoplasts/mL) were mixed with 50 µL of
180 solution C (room temperature), and a maximum of 15 µL DNA solution containing 2.5 µg of the
181 pLM-AMA15.0 plasmid and 5 µg of RT. The mixture was incubated on ice for 20 min. After
182 incubation, 2 mL of solution C were added, and after 5 min incubation at room temperature, 2

183 mL of solution B were added to the protoplast suspension. Finally, protoplasts were spread over
184 phleomycin-containing square plates (35 µg/mL) of *P. digitatum* minimal medium sucrose
185 (PdMMS) in the case of *P. digitatum,* or *Aspergillus* minimal medium sucrose (MMS) in the case
186 of *P. expansum.* As internal controls for transformation, we additionally inoculated
187 untransformed protoplasts on non-selective plates to test protoplasts viability (regeneration
188 control) and on selective plates as negative control. Plates were incubated at 25 ºC until
189 sporulated colonies were observed (approximately 12 or 7 days for *P. digitatum* or
190 *P. expansum*, respectively). A schematic representation of the protoplast transformation
191 protocol is shown in Fig. 1.

192 Transformants were purified by one colony streak to selective PDA plates and at least four
193 consecutive single colony streaks to non-selective PDA plates in order to (1) obtain monosporic
194 cultures, and (2) cure the strains from the plasmid and ensure the recycling of the system.
195 Genomic DNA of the transformants was isolated using the NZY Tissue gDNA Isolation kit
196 (Nzytech) and mutants were confirmed by PCR reactions (NZYTaq II DNA polymerase,
197 Nzytech) using the primers indicated in Table 1 and by Sanger sequencing. Finally, the verified
198 CRISPR/Cas9 mutants were plated on selection plates again to confirm their inability to grow in
199 the presence of the antibiotic, confirming the loss (and thus, not a random integration) of the
200 plasmid.

201 **2.4. Conidia production and germination**

202 In order to compare conidia production between the parental and mutant strains, 250 conidia
203 from *P. digitatum* CECT 20796, *P. expansum* CECT 20906, and *ΔwetA* mutants were
204 inoculated in the center of PDA plates and, after 7 days of growth, spores were collected in
205 sterile Milli-Q H_2O, filtered, counted with a hemacytometer and normalized to the surface of the
206 fungal colony. Assays were performed in technical triplicates.

207 Two different approaches were performed to evaluate and compare the conidial germination
208 rates between the parental and mutant strains. First, a final concentration of 10^6 conidia/mL
209 were inoculated in 100 µL 5% potato dextrose broth (PDB, Difco-BD Diagnostics) for 20 h in the
210 case of *P. digitatum* and 16 h in the case of *P. expansum,* at 25 ºC and 60 rpm. On the other
211 hand, a final concentration of 10^6 conidia/mL were inoculated in 100 µL sterile H_2O Milli-Q water
212 for 72 h at 25 ºC and 60 rpm. After each incubation time, samples were assessed for the
213 presence of non-germinated conidia, swollen conidia/germlings, and germ tubes. All treatments
214 were performed in technical triplicates.

215 In all cases, statistical differences between parental and mutant strains were assessed using a
216 Student's *t*-test ($p<0.05$).

217 **2.5. Antifungal activity assays**

218 Antifungal assays were performed in 96-well, flat-bottom microtiter plates (Nunc) as described
219 (Garrigues et al. 2018). Briefly, 50 µL of fungal conidia (5×10^4 conidia/mL) in 10% diluted PDB
220 and 0.02% (w/v) chloramphenicol were mixed with 50 µL of two-fold concentrated antifungal
221 proteins (AFPs) from serial twofold dilutions. Plates were statically incubated for 96 h at 25 °C.
222 Growth was determined every 24 h by measuring the optical density (OD) at 600 nm using
223 Spectrostar Nano microplate spectrophotometer (BMG labtech), and the OD_{600} mean and
224 standard deviation (SD) of three replicates were calculated. These experiments were repeated
225 three times. Minimum Inhibitory Concentration (MIC) is defined as the protein concentration that
226 completely inhibited growth in all the experiments.

227 **2.6. Fruit infection assays**

228 *P. digitatum* and *P. expansum* strains were inoculated on freshly harvested fruits of orange
229 (*Citrus sinensis* L. Osbeck cv Navel) and apples purchased in a local grocery (*Malus domestica*

230 cv Golden Delicious), respectively, as described (Ballester et al. 2014; González-Candelas et al.
231 2010). In brief, three replicates of five fruits were inoculated with 5 µL of conidial suspension (1
232 × 10^4 conidia/mL in oranges and 2.5 × 10^4 conidia/mL in apples) at four wounds around the
233 equator. Control mock-inoculations were carried out with 5 µL of sterile Milli-Q H_2O. After
234 inoculation, fruits were maintained at 20 °C and 90% relative humidity. Each inoculated wound
235 was scored daily for infection symptoms on consecutive days post inoculation (dpi). The
236 experiments were repeated at least two times.

237 **3. Results and Discussion**

238 **3.1. CRISPR/Cas9 was successfully applied to generate Δ*wetA* mutants in**
239 ***P. digitatum* and *P. expansum* through PMT.**

240 In this work, we developed protoplast generation and transformation protocols to genetically
241 modify both *P. digitatum* and *P. expansum* through CRISPR/Cas9 for the first time. Previously,
242 only ATMT protocols allowed the transformation and genetic modification of these two species
243 (Buron-Moles et al. 2012; Wang and Li 2008). However, ATMT typically results in (low copy)
244 genome integrations that often require selection markers for transformants selection, which can
245 be a limiting factor in case of multiple transformation events. On the other hand, PMT allows the
246 translocation of a high copy number of DNA molecules into the cells, which may result in higher
247 transformation rates (Weyda et al. 2017). Furthermore, PMT enables the transitive introduction
248 of non-integrative, self-replicating plasmids that can be cured after the genomic modification of
249 interest has been performed. Thus, it allows (i) the recycling of the system and (ii) an endless
250 number of genetic modifications without the limitation of selection markers.

251 In the present study, we applied the non-integrative self-replicating plasmid pLM-AMA15.0
252 (Supplementary Fig. S1) to genetically modify *P. digitatum* and *P. expansum* by means of
253 CRISPR/Cas9. As a test case, we targeted the *wetA* gene, which encodes a conidiophore

254 development-related transcription factor that is crucial for synthesis of cell wall layers that make
255 conidia mature and impermeable (Wang et al. 2015). Disruption of *wetA* has been reported to
256 generate white, cotton-like mutant colonies in several fungal species (Tao and Yu 2011; Wang
257 et al. 2015; Wu et al. 2018; Wu et al. 2017), making them easily distinguishable from their
258 parental strains, although other fungi e.g., *F. graminearum* Δ*wetA* mutants did not show
259 phenotypical differences compared to the wild type (Son et al. 2014).

260 After 12 and 7 days post-transformation of *P. digitatum* and *P. expansum,* respectively,
261 phleomycin-resistant colonies (Fig. 2A and Fig. 3A) were ready to be transferred, at least four
262 times, to non-selective plates in order to obtain monosporic cultures, and to induce the loss of
263 the plasmid and ensure the recycling of the system. This procedure generated *Penicillium*
264 strains that were again sensitive to the antibiotic used for transformant selection (data not
265 shown), as similarly reported for other CRISPR/Cas9-derived mutants (Pohl et al. 2016;
266 Salazar-Cerezo et al. 2020; Weyda et al. 2017), thus discarding the random integration of the
267 plasmid into the genome. Finally, the resulting *P. digitatum* and *P. expansum* transformants
268 were analyzed (Fig. 2B-C and Fig. 3B-C). Since the Cas9 cleavage efficiency through a gRNA
269 sequence is not yet well understood, and depends on several factors such as the genomic
270 region being targeted and the gRNA design (Katayama et al. 2016; Li et al. 2015), two different
271 gRNA sequences were designed and tested to disrupt *wetA* in both *Penicillium* species under
272 study. However, only one gRNA resulted in positive Δ*wetA* mutants (Table 1, and data not
273 shown). In case of *P. digitatum,* a genome editing efficiency of 10.1 ± 1.4% was reached with
274 the CRISPR/Cas9 system under study after several transformation experiments. Molecular
275 characterization of randomly chosen transformants showed that several strains underwent
276 NHEJ DNA repair mechanism (Pd_26, Pd_46, Pd_56), as depicted in Fig 2B-C. Sequencing
277 results of three independent white colonies demonstrated that all three had nucleotide deletions
278 within the *wetA* coding sequence, resulting in gene frameshift (Fig 2C, in yellow). Noteworthy,

279 one of our *P. digitatum* Δ*wetA* mutants presented a nucleotide deletion a few nucleotides
280 upstream of the gRNA complementary sequence (Pd_26, Fig. 2C). Similarly, in case of *P.*
281 *expansum*, an average genome editing efficiency of 12.7 ± 2.2% was reached with the pLM-
282 AMA15.0 Cas9 plasmid. Molecular characterization of transformants (Fig. 3B-C) showed that
283 both NHEJ (mutants Pe_04, Pe_20) and HR (Pe_16) occurred. In Pe_16, the complete Δ*wetA*
284 gene was removed by HR in the presence of RT (see also next section). Sequencing results of
285 two independent white colonies that underwent NHEJ (Pe_04, Pe_20) showed that all had
286 nucleotide deletions within the 20 bp sequence complementary to the gRNA targeting *wetA* (Fig
287 3C, in yellow). In addition, Pe_04 showed a nucleotide deletion a few nucleotides downstream
288 of the gRNA complementary sequence. In theory, Cas9-derived genetic modifications are
289 expected to occur within the 20 bp sequence complementary to the gRNA, and close to the
290 PAM sequence (Allen et al. 2019; Nødvig et al. 2015).These punctual nucleotide deletions in
291 off-target sites could be explained by the random nature of the NHEJ repair mechanism to
292 remedy DNA damage, which is not fully understood especially for the breaks inflicted by Cas9
293 (Allen et al. 2019).

294 The mutation rate of approx. 10-12% obtained for *P. digitatum* and *P. expansum* is comparable
295 to that obtained for other filamentous fungi such as *A. alternata* (Wenderoth et al. 2017), or
296 *P. subrubescens* (Salazar-Cerezo et al. 2020) and higher than that described for other fungi
297 e.g., *A. carbonarius* (Weyda et al. 2017). However, this efficiency was not as high as reported
298 for other filamentous fungi in which also CRISPR/Cas9 plasmids where used (Nødvig et al.
299 2015; Pohl et al. 2016; Song et al. 2018; Wang et al. 2021). In these studies, gene editing
300 efficiencies could vary between 23-97% depending on the fungus and the CRISPR/Cas9
301 approach. Many factors can (in)directly affect CRISPR/Cas9 genome editing, such as the
302 efficiency of the transformation process, the promoters driving the expression of *cas9* and the
303 gRNAs, *cas9* codon usage, the 20-nucleotide gRNA design, or the accessibility of the target

304 sequence, among others (Katayama et al. 2016; Li et al. 2015). These factors will be taken into
305 account to improve genome editing efficiency in both *P. digitatum* and *P. expansum.*

306 **3.2. Co-transformation of long homology-based repair templates does not increase**
307 **HDR over NHEJ**

308 In this study, we also tested if the presence of RTs would increase *P. digitatum* and
309 *P. expansum* preference for HDR over NHEJ. The NHEJ DNA repair mechanism mainly
310 involves the binding of the dimeric protein complex KU70/KU80 to the free DNA ends after
311 DSBs, resulting in random, error-prone DNA repair. In contrast, HDR-mediated recombination of
312 a homologous DNA sequence allows for precise genetic modifications and is more suited for
313 targeted genome editing (Snoek et al. 2009). The NHEJ is the dominant mechanism to repair
314 DSBs in filamentous fungi (Haarmann et al. 2008; Li et al. 2010; Snoek et al. 2009; Xu et al.
315 2014). Thus, reaching efficient levels of HDR is challenging in wild-type fungal strains in which
316 the NHEJ repair pathway has not been inactivated. The addition of homology-based RTs to
317 CRISPR/Cas9 transformation events has been shown to induce HDR-based mutations in some
318 fungal species without the necessity to previously inactivate the NHEJ pathway (Al Abdallah et
319 al. 2017; Foster et al. 2018; Jan-Vonk et al. 2019). In this work, we constructed RTs using
320 approx. 1.2 kb complementary DNA arms to both 5' and 3' flanking regions of the *wetA* genes in
321 *P. digitatum* and *P. expansum,* since previous studies demonstrated that Cas9-derived DSBs
322 could be repaired by homology arms of this size in other *Penicillium* species (Pohl et al. 2016;
323 Salazar-Cerezo et al. 2020). Molecular characterization of *P. digitatum* transformants through
324 PCR showed that, despite the co-transformation of the CRISPR/Cas9 plasmid with high
325 amounts of homology-based RT (≈ 5 µg), none of the phleomycin-resistant transformants
326 analyzed showed a band size of around 2.4 kb indicative of clean deletion of *wetA* gene through
327 HR (Fig. 2B and data not shown). In the case of *P. expansum*, molecular characterization of
328 phleomycin-resistant transformants showed that only one of the mutants analyzed (Pe_16)

329 showed a band of 2.6 kb indicative of clean deletion of *wetA* through HR in the presence of RT
330 (Fig. 3B). However, despite the presence of RT, there is still a general preference for NHEJ over
331 HDR DNA repair system in both organisms (Fig. 2, Fig. 3, and data not shown).

332 A common approach to improve CRISPR/Cas9 efficiency through HDR in filamentous fungi is
333 the construction of *ku70/ku80* knockouts, leading to (partial) inactivation of the NHEJ repair
334 pathway. It has been shown that the disruption of these genes in filamentous fungi could
335 significantly improve the efficiency of HR up to 100% (Haarmann et al. 2008; Li et al. 2010;
336 Matsu-Ura et al. 2015; Pohl et al. 2016; Schuster et al. 2016; Xu et al. 2014). Based on this, and
337 taking into account our own results, the application of the CRISPR/Cas9 technology in NHEJ-
338 deficient *P. digitatum* and *P. expansum* could help improve the already obtained CRISPR/Cas9
339 efficiency rates, and will be addressed in the future.

340 **3.3. Disruption of *wetA* in *P. digitatum* and *P. expansum* results in reduction of axenic**
341 **growth, differential pathogenicity and altered conidiogenesis and germination.**

342 The *wetA* gene, together with *brlA* and *abaA,* defines a central regulatory pathway that governs
343 conidiation-specific gene expression and determine conidiophore formation and spore
344 maturation (Park and Yu 2012). Several studies have already shown that *wetA* deletion totally
345 blocks conidia pigmentation, resulting in conidia with albino phenotypes (Tao and Yu 2011;
346 Wang et al. 2015; Wu et al. 2018; Wu et al. 2017). Molecular characterization of phleomycin-
347 resistant transformants obtained by CRISPR/Cas9 demonstrated the disruption of the *wetA*
348 gene in both *P. digitatum* and *P. expansum* (Fig. 2 and Fig. 3). From this point onwards, the
349 molecularly verified Δ*wetA* mutants of *P. digitatum* Pd_46, Pd_26, and Pd_56 (Fig. 2) will be
350 referred to as Δ*PdwetA*_46, Δ*PdwetA*_26, and Δ*PdwetA*_56, respectively. Similarly, the verified
351 Δ*wetA* mutants of *P. expansum* Pe_04, Pe_16 and Pe_20 (Fig. 3) will be referred to as
352 Δ*PewetA*_04, Δ*PewetA*_16, and Δ*PewetA*_20. Phenotypic characterization of *P. digitatum* and

353 *P. expansum* Δ*wetA* mutants on solid plates confirmed the expected albino phenotypes (Fig.
354 4A). Additionally, growth of three independent Δ*wetA* mutants from each strain showed delayed
355 growth on PDA plates compared to their corresponding wild-type strains (Fig. 4B).

356 In filamentous fungi, the involvement of *wetA* in pathogenicity and virulence seems to be
357 species-dependent. For example, *wetA* disruption has been described to negatively affect
358 pathogenicity and virulence in the entomopathogenic fungus *Beauveria bassiana* (Li et al.
359 2015). In contrast, virulence of *F. graminearum* Δ*wetA* mutants did not significantly differ from
360 the original strain (Son et al. 2014). Our pathogenicity assays revealed that *P. digitatum* Δ*wetA*
361 mutants showed significantly reduced pathogenicity compared to that of the wild type on orange
362 fruits ($p<0.05$) (Fig. 4 C-D). This is in discordance with a previously published work in which
363 other *P. digitatum* Δ*wetA* mutants were reported to show similar pathogenicity and virulence to
364 that of their corresponding parental strain (Wang et al. 2015). However, in our study, a different
365 *P. digitatum* strain, lower inoculum dose, and an alternative pathosystem were used, which
366 could be the main reasons for these discrepancies. In case of *P. expansum*, although there
367 seems to be a slight tendency of reduced pathogenicity in the Δ*wetA* mutants compared to the
368 control, this is not statistically significant (Fig. 4 E-F).

369 Null *wetA* mutants from both *P. digitatum* and *P. expansum* showed reduced conidia production
370 ability after 7 days of growth on PDA plates, although this reduction was only statistically
371 significant in the case of *P. expansum* Δ*wetA* mutants (Fig. 5A). Surprisingly, germination rates
372 of independent Δ*wetA* mutants from both *P. digitatum* and *P. expansum* was increased in liquid
373 PDB medium (Fig. 5B) and in sterile water (Fig. 5C).

374 A previous study reported decreased germination rate in a different strain of *P. digitatum wetA*
375 mutant measured on solid PDA plates (Wang et al. 2015). In that study, 44% and 97% of wild-
376 type *P. digitatum* PdKH8 conidia germinated at 8 h and 12 h after incubation in PDA,
377 respectively, while in the Δ*PdwetA* mutants, only approximately 7% and 42% of conidia

378 germinated at these two corresponding time points. In our case, we measured the germination
379 rate in a different medium (solid vs. liquid) and in a different *P. digitatum* strain, which could
380 (partially) explain these differences. In our study, only around 30% of the wild-type spores
381 completely germinated after 20 h of incubation in liquid PDB, while between 60-70% of the
382 Δ*PdwetA* conidia had already germinated (Fig. 5B, left panel). These results were also
383 comparable in case of *P. expansum* Δ*wetA* mutants, in which the amount of conidia was also
384 significantly reduced after 16 h incubation in PDB, correlating with an increase in the amount of
385 germ tubes compared to the parental strain CMP-1 (Fig. 5B, right panel). Around 30% of the
386 CMP-1 wild-type spores completely germinated after 16 h of incubation in liquid PDB, whereas
387 between 40-60% of the Δ*PewetA* conidia had already germinated (Fig. 5B, right panel).

388 In order to further confirm the increased germination rate of the mutants, we also tested their
389 germination ability in sterile H_2O, which is an alternative liquid matrix where germination is more
390 restricted due to lack of nutrients. Results showed that after 72 h incubation, there was a
391 significant reduction of spores and a significant increase of germ tubes in the case of
392 *P. digitatum* Δ*wetA* mutants compared to the parental strain PHI26 (Fig. 5C, left panel). In
393 parallel, results of *P. expansum* Δ*wetA* strains also showed an increased germination rate of
394 these mutants in H_2O. The amount of non-germinated spores of the Δ*wetA* strains was
395 significantly reduced, correlating with a significant increase in the amount of germlings and germ
396 tubes compared to the wild-type strain (Fig. 5, right panel). It is noteworthy that no germ tubes
397 of the parental strains PHI26 or CMP-1 were present in the water samples after 72 h incubation
398 time, thus confirming the increased germination ability of null *wetA* mutants in both species.

399 **3.4. *P. digitatum* and *P. expansum* Δ*wetA* mutants show differential sensitivity to**
400 **distinct fungal antifungal proteins (AFPs)**

401 Apart from conidia pigmentation, *wetA* gene has also been reported to play a role in the integrity
402 of the conidia cell wall (Park and Yu 2012; Wang et al. 2015), which acts as a key defense to
403 withstand stressing agents and harsh environmental conditions (Fuchs and Mylonakis 2009). A
404 previously published study already demonstrated altered tolerance of *P. digitatum* Δ*wetA*
405 mutants to oxidative compounds (e.g., menadione, H_2O_2) osmotic agents (NaCl) and detergents
406 (sodium dodecyl sulfate (SDS)) (Wang et al. 2015). However, no information about the putative
407 altered tolerance to stressing compounds in *P. expansum* Δ*wetA* mutants is available to date.

408 In this work, we tested whether *wetA* disruption might affect *P. digitatum* and *P. expansum*
409 susceptibility to the so called fungal antifungal proteins (AFPs). AFPs are small, cationic
410 cysteine-rich proteins that are often secreted in large amounts by filamentous ascomycetes and
411 are active against a wide range of fungi (Hegedüs and Marx 2013). AFPs have become
412 interesting antifungals to be applied in agriculture, medicine and in the food industry (Marx et al.
413 2008; Delgado et al. 2016; Garrigues et al. 2018; Martínez-Culebras et al. 2021; Tóth et al.
414 2020), although their modes of action are still poorly understood. PeAfpA from *P. expansum* and
415 PdAfpB from *P. digitatum* are among the most active AFPs described to date (Garrigues et al.
416 2018; Garrigues et al. 2017). Their antifungal efficacy has been demonstrated *in vitro* against a
417 wide range of opportunistic human, animal, plant and foodborne pathogenic fungi (Garrigues et
418 al. 2018; Garrigues et al. 2017), and *in vivo* against the economically relevant phytopathogens
419 *P. digitatum, B. cinerea* and *P. expansum* during infection in oranges, tomato plants and apples,
420 respectively (Gandía et al. 2020; Garrigues et al. 2018).

421 Growth inhibition assays of *P. expansum* Δ*wetA* mutants by PeAfpA and PdAfpB (Fig. 6A)
422 showed that there is no differential susceptibility between the parental CMP-1 and the mutant
423 strains for both of the two AFPs under study (MIC_{PeAfpA} = 2 µg/mL; MIC_{PdAfpB} = 8 µg/mL). In

424 contrast, whereas *P. digitatum* Δ*wetA* mutants showed similar tolerance to PeAfpA to that of the
425 reference strain PHI26 (MIC_{PeAfpA} = 1 µg/mL), they showed increased tolerance to PdAfpB
426 ($MIC_{PdAfpB/PHI26}$ = 4 µg/mL; $MIC_{PdAfpB/Pd\Delta wetA}$ = 8 µg/mL) (Fig. 6B). These results would suggest
427 that: (i) *wetA* deletion might differentially affect *P. expansum* and *P. digitatum* conidia*;* and/or
428 that (ii) there is a differential mode of action between PeAfpA and PdAfpB in *P. digitatum*. We
429 have already demonstrated that PdAfpB acts through a three-step killing mechanism in this
430 fungus, in which the conidia cell wall has a key role in the initial stage of protein-cell interaction
431 (Bugeda et al. 2020). However, there is no published information on the mode of action of
432 PeAfpA to date. Studies on the mode of action of PeAfpA are in progress and will help validate
433 this hypothesis.

434 **4. Conclusions**

435 In this study, we describe effective protoplast generation and transformation protocols for the
436 implementation of the CRISPR/Cas9 genome editing technology in the phytopathogenic fungi
437 *P. digitatum* and *P. expansum* for the first time. Although there is still room for improvement, the
438 CRISPR/Cas9 system was successfully applied through a recyclable AMA1-based plasmid to
439 disrupt the *wetA* gene in both species, and phenotypic characterization of these mutants was
440 performed. With this work, we expand the repertoire of genetic engineering tools available for
441 these two important postharvest pathogenic species, and open up new possibilities to study
442 gene function without the limitation of selection markers. In addition, the methods presented
443 here could probably be adapted to other economically relevant phytopathogenic fungi, for which
444 the availability of genetic modification tools is often limited.

445 **5. Declarations**

446 **Funding:** This work was supported by PROMETEO/2018/066 from 'Conselleria d'Educació'
447 (Generalitat Valenciana, Comunitat Valenciana, Spain). SG holds a 'Juan de la Cierva

Incorporación' grant (IJC2020-042749-I) from the Spanish 'Ministerio de Ciencia e Innovación', funded by The European Union– NextGenerationEU.

Acknowledgements: We acknowledge the group of Dr. Arnold J.M. Driessen for kindly providing the plasmid pLM-AMA15.0, and Zara Sáez for her excellent technical assistance.

Author Contributions: All authors conceived and designed the study. SG performed the experiments and wrote the first draft of the manuscript. PM and JFM reviewed and edited the manuscript. All authors read and approved the final manuscript.

Conflicts of interest/Competing interests: The authors have no conflicts of interest to declare that are relevant to the content of this article.

Availability of data and material: all data generated or analyzed during this study are included in this published article.

Code availability: Not applicable.

6. References

Al Abdallah Q, Ge W, Fortwendel-Jarrod R, Mitchell-Aaron P (2017) A simple and universal system for gene manipulation in *Aspergillus fumigatus*: In vitro-assembled Cas9-guide RNA ribonucleoproteins coupled with microhomology repair templates. mSphere 2: e00446-00417 doi: 10.1128/mSphere.00446-17

Allen F, Crepaldi L, Alsinet C, Strong AJ, Kleshchevnikov V, De Angeli P, Páleníková P, Khodak A, Kiselev V, Kosicki M, Bassett AR, Harding H, Galanty Y, Muñoz-Martínez F, Metzakopian E, Jackson SP, Parts L (2019) Predicting the mutations generated by repair of Cas9-induced double-strand breaks. Nat Biotechnol 37: 64-72 doi: 10.1038/nbt.4317

Arazoe T, Miyoshi K, Yamato T, Ogawa T, Ohsato S, Arie T, Kuwata S (2015) Tailor-made CRISPR/Cas system for highly efficient targeted gene replacement in the rice blast fungus. Biotechnol Bioeng 112: 2543-2549 doi: 10.1002/bit.25662

Ballester A-R, López-Pérez M, de la Fuente B, González-Candelas L (2019) Functional and pharmacological analyses of the role of *Penicillium digitatum* proteases on virulence. Microorganisms 7: 7 doi: 710.3390/microorganisms7070198

Ballester A-R, Marcet-Houben M, Levin E, Sela N, Selma-Lázaro C, Carmona L, Wisniewski M, Droby S, González-Candelas L, Gabaldón T (2014) Genome, transcriptome, and functional analyses of *Penicillium expansum* provide new insights into secondary

480 metabolism and pathogenicity. Mol Plant-Microbe Interact 28: 232-248 doi:
481 10.1094/mpmi-09-14-0261-fi
482 Bugeda A, Garrigues S, Gandía M, Manzanares P, Marcos JF, Coca M (2020) The antifungal
483 protein AfpB induces regulated cell death in its parental fungus *Penicillium digitatum*.
484 mSphere 5: e00595-00520 doi: 10.1128/mSphere.00595-20
485 Buron-Moles G, López-Pérez M, González-Candelas L, Viñas I, Teixidó N, Usall J, Torres R
486 (2012) Use of GFP-tagged strains of *Penicillium digitatum* and *Penicillium expansum* to
487 study host-pathogen interactions in oranges and apples. Int J Food Microbiol 160: 162-
488 170 doi: 10.1016/j.ijfoodmicro.2012.10.005
489 Costa JH, Bazioli JM, de Moraes Pontes JG, Fill TP (2019) *Penicillium digitatum* infection
490 mechanisms in citrus: what do we know so far? Fungal Biol 123: 584-593 doi:
491 10.1016/j.funbio.2019.05.004
492 Chen Y, Li B, Xu X, Zhang Z, Tian S (2018) The pH-responsive PacC transcription factor plays
493 pivotal roles in virulence and patulin biosynthesis in *Penicillium expansum*. Environ
494 Microbiol 20: 4063-4078 doi: 10.1111/1462-2920.14453
495 Davis AJ, Chen DJ (2013) DNA double strand break repair via non-homologous end-joining.
496 Transl Cancer Res 2: 3 doi: 210.3978/j.issn.2218-676X.2013.04.02.
497 de Ramón-Carbonell M, Sánchez-Torres P (2017) The transcription factor PdSte12 contributes
498 to *Penicillium digitatum* virulence during citrus fruit infection. Postharvest Biol Technol
499 125: 129-139 doi: 10.1016/j.postharvbio.2016.11.012
500 Delgado J, Owens RA, Doyle S, Asensio MA, Núñez F (2016) Antifungal proteins from moulds:
501 analytical tools and potential application to dry-ripened foods. Appl Microbiol Biotechnol
502 100: 6991-7000 doi: 10.1007/s00253-016-7706-2
503 Doench JG, Hartenian E, Graham DB, Tothova Z, Hegde M, Smith I, Sullender M, Ebert BL,
504 Xavier RJ, Root DE (2014) Rational design of highly active sgRNAs for CRISPR-Cas9–
505 mediated gene inactivation. Nat Biotechnol 32: 1262-1267 doi: 10.1038/nbt.3026
506 Engler C, Gruetzner R, Kandzia R, Marillonnet S (2009) Golden gate shuffling: a one-pot DNA
507 shuffling method based on type IIs restriction enzymes. PLOS ONE 4: e5553 doi:
508 10.1371/journal.pone.0005553
509 Foster AJ, Martin-Urdiroz M, Yan X, Wright HS, Soanes DM, Talbot NJ (2018) CRISPR-Cas9
510 ribonucleoprotein-mediated co-editing and counterselection in the rice blast fungus. Sci
511 Rep 8: 14355 doi: 10.1038/s41598-018-32702-w
512 Fuchs B, Mylonakis E (2009) Our paths might cross: the role of the fungal cell wall integrity
513 pathway in stress response and cross talk with other stress response pathways.
514 Eukaryot Cell 8: 1616-1625 doi: 10.1128/ec.00193-09
515 Gandía M, Garrigues S, Bolós B, Manzanares P, Marcos JF (2019a) The Myosin motor domain-
516 containing chitin synthases are involved in cell wall integrity and sensitivity to antifungal
517 proteins in *Penicillium digitatum*. Front Microbiol doi: 1010.3389/fmicb.2019.02400
518 Gandía M, Garrigues S, Hernanz-Koers M, Manzanares P, Marcos JF (2019b) Differential roles,
519 crosstalk and response to the antifungal protein AfpB in the three mitogen-activated
520 protein kinases (MAPK) pathways of the citrus postharvest pathogen *Penicillium*
521 *digitatum*. Fungal Genet Biol 124: 17-28 doi: 10.1016/j.fgb.2018.12.006
522 Gandía M, Harries E, Marcos JF (2014) The myosin motor domain-containing chitin synthase
523 PdChsVII is required for development, cell wall integrity and virulence in the citrus
524 postharvest pathogen *Penicillium digitatum*. Fungal Genet Biol 67: 58-70 doi:
525 10.1016/j.fgb.2014.04.002
526 Gandía M, Monge A, Garrigues S, Orozco H, Giner-Llorca M, Marcos JF, Manzanares P (2020)
527 Novel insights in the production, activity and protective effect of *Penicillium expansum*
528 antifungal proteins. Int J Biol Macromol 164: 3922-3931 doi:
529 10.1016/j.ijbiomac.2020.08.208

530 Gardiner DM, Kazan K (2018) Selection is required for efficient Cas9-mediated genome editing
531 in *Fusarium graminearum*. Fungal Biol 122: 131-137 doi: 10.1016/j.funbio.2017.11.006
532 Garrigues S, Gandía M, Castillo L, Coca M, Marx F, Marcos JF, Manzanares P (2018) Three
533 antifungal proteins from *Penicillium expansum*: different patterns of production and
534 antifungal activity. Front Microbiol 910.3389/fmicb.2018.02370
535 Garrigues S, Gandía M, Popa C, Borics A, Marx F, Coca M, Marcos JF, Manzanares P (2017)
536 Efficient production and characterization of the novel and highly active antifungal protein
537 AfpB from *Penicillium digitatum*. Sci Rep 7: 14663 doi: 10.1038/s41598-017-15277-w
538 Garrigues S, Marcos JF, Manzanares P, Gandía M (2020) A novel secreted cysteine-rich
539 anionic (Sca) protein from the citrus postharvest pathogen *Penicillium digitatum*
540 enhances virulence and modulates the activity of the Antifungal Protein B (AfpB). J
541 Fungi doi: 610.3390/jof6040203
542 González-Candelas L, Alamar S, Sánchez-Torres P, Zacarías L, Marcos JF (2010) A
543 transcriptomic approach highlights induction of secondary metabolism in citrus fruit in
544 response to *Penicillium digitatum* infection. BMC Plant Biol 10: 194 doi: 10.1186/1471-
545 2229-10-194
546 Haarmann T, Lorenz N, Tudzynski P (2008) Use of a nonhomologous end joining deficient
547 strain (Δ*ku70*) of the ergot fungus *Claviceps purpurea* for identification of a nonribosomal
548 peptide synthetase gene involved in ergotamine biosynthesis. Fungal Genet Biol 45: 35-
549 44 doi: 10.1016/j.fgb.2007.04.008
550 Harries E, Gandía M, Carmona L, Marcos JF (2015) The *Penicillium digitatum* protein O-
551 mannosyltransferase Pmt2 is required for cell wall integrity, conidiogenesis, virulence
552 and sensitivity to the antifungal peptide PAF26. Mol Plant Pathol 16: 748-761 doi:
553 10.1111/mpp.12232
554 Hegedüs N, Marx F (2013) Antifungal proteins: More than antimicrobials? Fungal Biol Rev 26:
555 132-145 doi: 10.1016/j.fbr.2012.07.002
556 Jan-Vonk P, Escobar N, Wösten HAB, Lugones LG, Ohm RA (2019) High-throughput targeted
557 gene deletion in the model mushroom *Schizophyllum commune* using pre-assembled
558 Cas9 ribonucleoproteins. Sci Rep 9: 7632 doi: 10.1038/s41598-019-44133-2
559 Jinek M, Chylinski K, Fonfara I, Hauer M, Doudna JA, Charpentier E (2012) A programmable
560 dual-RNA-guided DNA endonuclease in adaptive bacterial immunity. Science 337: 816-
561 821 doi: 10.1126/science.1225829
562 Julca I, Droby S, Sela N, Marcet-Houben M, Gabaldón T (2016) Contrasting genomic diversity
563 in two closely related postharvest pathogens: *Penicillium digitatum* and *Penicillium*
564 *expansum*. Genome Biol Evol 8: 218-227 doi: 10.1093/gbe/evv252
565 Katayama T, Tanaka Y, Okabe T, Nakamura H, Fujii W, Kitamoto K, Maruyama J-I (2016)
566 Development of a genome editing technique using the CRISPR/Cas9 system in the
567 industrial filamentous fungus *Aspergillus oryzae*. Biotechnol Lett 38: 637-642 doi:
568 10.1007/s10529-015-2015-x
569 Kowalczyk JE, Lubbers RJM, Peng M, Battaglia E, Visser J, de Vries RP (2017) Combinatorial
570 control of gene expression in *Aspergillus niger* grown on sugar beet pectin. Sci Rep 7:
571 12356 doi: 10.1038/s41598-017-12362-y
572 Králová M, Bergougnoux V, Frébort I (2021) CRISPR/Cas9 genome editing in ergot fungus
573 *Claviceps purpurea*. J Biotechnol 325: 341-354 doi: 10.1016/j.jbiotec.2020.09.028
574 Kun RS, Gomes ACS, Hildén KS, Salazar Cerezo S, Mäkelä MR, de Vries RP (2019)
575 Developments and opportunities in fungal strain engineering for the production of novel
576 enzymes and enzyme cocktails for plant biomass degradation. Biotechnol Adv 37:
577 107361 doi: 10.1016/j.biotechadv.2019.02.017
578 Leisen T, Bietz F, Werner J, Wegner A, Schaffrath U, Scheuring D, Willmund F, Mosbach A,
579 Scalliet G, Hahn M (2020) CRISPR/Cas with ribonucleoprotein complexes and
580 transiently selected telomere vectors allows highly efficient marker-free and multiple

581 genome editing in *Botrytis cinerea*. PLOS Pathog 16: e1008326 doi:
582 10.1371/journal.ppat.1008326
583 Li B, Chen Y, Zhang Z, Qin G, Chen T, Tian S (2020) Molecular basis and regulation of
584 pathogenicity and patulin biosynthesis in *Penicillium expansum*. Compr Rev Food Sci
585 Food Saf 19: 3416-3438 doi: 10.1111/1541-4337.12612
586 Li Z-H, Du C-M, Zhong Y-H, Wang T-H (2010) Development of a highly efficient gene targeting
587 system allowing rapid genetic manipulations in *Penicillium decumbens*. Appl Microbiol
588 Biotechnol 87: 1065-1076 doi: 10.1007/s00253-010-2566-7
589 Li Z, Yao G, Wu R, Gao L, Kan Q, Liu M, Yang P, Liu G, Qin Y, Song X, Zhong Y, Fang X, Qu Y
590 (2015) Synergistic and dose-controlled regulation of cellulase gene expression in
591 *Penicillium oxalicum*. PLOS Genet 11: e1005509 doi: 10.1371/journal.pgen.1005509
592 Liu R, Chen L, Jiang Y, Zhou Z, Zou G (2015) Efficient genome editing in filamentous fungus
593 *Trichoderma reesei* using the CRISPR/Cas9 system. Cell Discov 1: 15007 doi:
594 10.1038/celldisc.2015.7
595 Liu Y, Galani Yamdeu JH, Gong YY, Orfila C (2020) A review of postharvest approaches to
596 reduce fungal and mycotoxin contamination of foods. Compr Rev Food Sci Food Saf 19:
597 1521-1560 doi: 10.1111/1541-4337.12562
598 Marcet-Houben M, Ballester A-R, de la Fuente B, Harries E, Marcos JF, González-Candelas L,
599 Gabaldón T (2012) Genome sequence of the necrotrophic fungus *Penicillium digitatum*,
600 the main postharvest pathogen of citrus. BMC Genom 13: 646 doi: 10.1186/1471-2164-
601 13-646
602 Martínez-Culebras PV, Gandía M, Boronat A, Marcos JF, Manzanares P (2021) Differential
603 susceptibility of mycotoxin-producing fungi to distinct antifungal proteins (AFPs). Food
604 Microbiol 97: 103760 doi: 10.1016/j.fm.2021.103760
605 Marx F, Binder U, Leiter É, Pócsi I (2008) The *Penicillium chrysogenum* antifungal protein PAF,
606 a promising tool for the development of new antifungal therapies and fungal cell biology
607 studies. Cell Mol Life Sci 65: 445-454 doi: 10.1007/s00018-007-7364-8
608 Matsu-Ura T, Baek M, Kwon J, Hong C (2015) Efficient gene editing in *Neurospora crassa* with
609 CRISPR technology. Fungal Biol Biotechnol 2: 4 doi: 10.1186/s40694-015-0015-1
610 Morales H, Marín S, Rovira A, Ramos AJ, Sanchis V (2007) Patulin accumulation in apples by
611 *Penicillium expansum* during postharvest stages. Lett Appl Microbiol 44: 30-35 doi:
612 10.1111/j.1472-765X.2006.02035.x
613 Mózsik L, Hoekzema M, de Kok NAW, Bovenberg RAL, Nygård Y, Driessen AJM (2021)
614 CRISPR-based transcriptional activation tool for silent genes in filamentous fungi. Sci
615 Rep 11: 1118 doi: 10.1038/s41598-020-80864-3
616 Nødvig CS, Nielsen JB, Kogle ME, Mortensen UH (2015) A CRISPR-Cas9 system for genetic
617 engineering of filamentous fungi. PLOS ONE 10: e0133085 doi:
618 10.1371/journal.pone.0133085
619 Park H-S, Yu J-H (2012) Genetic control of asexual sporulation in filamentous fungi. Curr Opin
620 Microbiol 15: 669-677 doi: 10.1016/j.mib.2012.09.006
621 Pohl C, Kiel JAKW, Driessen AJM, Bovenberg RAL, Nygård Y (2016) CRISPR/Cas9 based
622 genome editing of *Penicillium chrysogenum*. ACS Synth Biol 5: 754-764 doi:
623 10.1021/acssynbio.6b00082
624 Prade RA, Timberlake WE (1994) The *Penicillium chrysogenum* and *Aspergillus nidulans wetA*
625 developmental regulatory genes are functionally equivalent. Mol Gen Genet 244: 539-
626 547 doi: 10.1007/bf00583905
627 Salazar-Cerezo S, Kun RS, de Vries RP, Garrigues S (2020) CRISPR/Cas9 technology enables
628 the development of the filamentous ascomycete fungus *Penicillium subrubescens* as a
629 new industrial enzyme producer. Enzyme Microb Technol 133: 109463 doi:
630 10.1016/j.enzmictec.2019.109463

631 Schuster M, Schweizer G, Reissmann S, Kahmann R (2016) Genome editing in *Ustilago maydis*
632 using the CRISPR–Cas system. Fungal Genet Biol 89: 3-9 doi:
633 10.1016/j.fgb.2015.09.001
634 Seekles SJ, Teunisse PPP, Punt M, van den Brule T, Dijksterhuis J, Houbraken J, Wösten HAB,
635 Ram AFJ (2021) Preservation stress resistance of melanin deficient conidia from
636 *Paecilomyces variotii* and *Penicillium roqueforti* mutants generated via CRISPR/Cas9
637 genome editing. Fungal Biol Biotechnol 8: 4 doi: 10.1186/s40694-021-00111-w
638 Snoek ISI, van der Krogt ZA, Touw H, Kerkman R, Pronk JT, Bovenberg RAL, van den Berg
639 MA, Daran JM (2009) Construction of an *hdfA Penicillium chrysogenum* strain impaired
640 in non-homologous end-joining and analysis of its potential for functional analysis
641 studies. Fungal Genet Biol 46: 418-426 doi: 10.1016/j.fgb.2009.02.008
642 Snowdon AL (1988) A review of the nature and causes of post-harvest deterioration in fruits and
643 vegetables, with especial reference to those in international trade. In: Houghton DR,
644 Smith RN, Eggins HOW (eds) Biodeterioration 7. Springer Netherlands, Dordrecht, pp.
645 585-602.
646 Son H, Kim M-G, Min K, Lim JY, Choi GJ, Kim J-C, Chae S-K, Lee Y-W (2014) WetA is required
647 for conidiogenesis and conidium maturation in the ascomycete fungus *Fusarium*
648 *graminearum*. Eukaryot Cell 13: 87-98 doi: 10.1128/ec.00220-13
649 Son Y-E, Park H-S (2021) Genetic manipulation and transformation methods for *Aspergillus*
650 spp. Mycobiology 49: 95-104 doi: 10.1080/12298093.2020.1838115
651 Song L, Ouedraogo J-P, Kolbusz M, Nguyen TTM, Tsang A (2018) Efficient genome editing
652 using tRNA promoter-driven CRISPR/Cas9 gRNA in *Aspergillus niger*. PLOS ONE 13:
653 e0202868 doi: 10.1371/journal.pone.0202868
654 Tao L, Yu J-H (2011) AbaA and WetA govern distinct stages of *Aspergillus fumigatus*
655 development. Microbiology 157: 313-326 doi: 10.1099/mic.0.044271-0
656 Tóth L, Boros É, Poór P, Ördög A, Kele Z, Váradi G, Holzknecht J, Bratschun-Khan D, Nagy I,
657 Tóth GK, Rákhely G, Marx F, Galgóczy L (2020) The potential use of the *Penicillium*
658 *chrysogenum* antifungal protein PAF, the designed variant PAFopt and its γ-core peptide
659 Pγopt in plant protection. Microb Biotechnol 13: 1403-1414 doi: 10.1111/1751-
660 7915.13559
661 Valente S, Piombo E, Schroeckh V, Meloni GR, Heinekamp T, Brakhage AA, Spadaro D (2021)
662 CRISPR-Cas9-based discovery of the verrucosidin biosynthesis gene cluster in
663 *Penicillium polonicum*. Front Microbiol 1210.3389/fmicb.2021.660871
664 Vilanova L, Viñas I, Torres R, Usall J, Jauset AM, Teixidó N (2012) Infection capacities in the
665 orange-pathogen relationship: compatible (*Penicillium digitatum*) and incompatible
666 (*Penicillium expansum*) interactions. Food Microbiol 29: 56-66 doi:
667 10.1016/j.fm.2011.08.016
668 Wang J-Y, Li H-Y (2008) *Agrobacterium tumefaciens*-mediated genetic transformation of the
669 phytopathogenic fungus *Penicillium digitatum*. J Zhejiang Univ Sci B 9: 823-828 doi:
670 10.1631/jzus.B0860006
671 Wang M, Sun X, Zhu C, Xu Q, Ruan R, Yu D, Li H (2015) *PdbrlA, PdabaA* and *PdwetA* control
672 distinct stages of conidiogenesis in *Penicillium digitatum*. Res Microbiol 166: 56-65 doi:
673 10.1016/j.resmic.2014.12.003
674 Wang Q, Coleman JJ (2019) Progress and challenges: development and implementation of
675 CRISPR/Cas9 technology in filamentous fungi. Comput Struct Biotechnol J 17: 761-769
676 doi: 10.1016/j.csbj.2019.06.007
677 Wang Q, Zhao Q, Liu Q, He X, Zhong Y, Qin Y, Gao L, Liu G, Qu Y (2021) CRISPR/Cas9-
678 mediated genome editing in *Penicillium oxalicum* and *Trichoderma reesei* using 5S
679 rRNA promoter-driven guide RNAs. Biotechnol Lett 43: 495-502 doi: 10.1007/s10529-
680 020-03024-7

681 Wenderoth M, Pinecker C, Voß B, Fischer R (2017) Establishment of CRISPR/Cas9 in
682 *Alternaria alternata*. Fungal Genet Biol 101: 55-60 doi: 10.1016/j.fgb.2017.03.001
683 Weyda I, Yang L, Vang J, Ahring BK, Lübeck M, Lübeck PS (2017) A comparison of

Primer ID	Use [a]	Sequence (5'-3') [b]	Target organism	Description [c]

684 *Agrobacterium*-mediated transformation and protoplast-mediated transformation with
685 CRISPR-Cas9 and bipartite gene targeting substrates, as effective gene targeting tools
686 for *Aspergillus carbonarius*. J Microbiol Methods 135: 26-34 doi:
687 10.1016/j.mimet.2017.01.015
688 Wright WD, Shah SS, Heyer WD (2018) Homologous recombination and the repair of DNA
689 double-strand breaks. J Biol Chem 293: 10524-10535 doi: 10.1074/jbc.TM118.000372
690 Wu M-Y, Mead ME, Lee M-K, Ostrem-Loss EM, Kim S-C, Rokas A, Yu J-H (2018) Systematic
691 dissection of the evolutionarily conserved WetA developmental regulator across a genus
692 of filamentous fungi. mBio 9: e01130-01118 doi: 10.1128/mBio.01130-18
693 Wu M-Y, Mead ME, Kim S-C, Rokas A, Yu J-H (2017) WetA bridges cellular and chemical
694 development in *Aspergillus flavus*. PLOS ONE 12: e0179571 doi:
695 10.1371/journal.pone.0179571
696 Xu Q, Zhu C-y, Wang M-s, Sun X-p, Li H-y (2014) Improvement of a gene targeting system for
697 genetic manipulation in *Penicillium digitatum*. J Zhejiang Univ Sci B 15: 116-124 doi:
698 10.1631/jzus.B1300213
699 Zhang T, Sun X, Xu Q, Candelas LG, Li H (2013) The pH signaling transcription factor PacC is
700 required for full virulence in *Penicillium digitatum*. Appl Microbiol Biotechnol 97: 9087-
701 9098 doi: 10.1007/s00253-013-5129-x
702

703

704 **7. Tables**

OJM654	F	CGACTCGGTGCCACTTTTTC	*E. coli*	plasmid screening
OJM655	R	CATCCATACTCCATCCTTCCC	*E. coli*	plasmid screening
OJM670	F	ATGGTCTCACCGAGAAGGACTGATGAGTCCGTGAGGACGAAACGAG	*P. expansum*	gRNA construction
OJM671	R	ATGGTCTCTAAACCCGACATGTCGTAGGAAGGAGACGAGCTTACTCGTTTCGTCCTCACGGACTCA	*P. expansum*	gRNA construction
OJM672	F	ATGGTCTCACCGAGCGAACCTGATGAGTCCGTGAGGACGAAACGAG	*P. digitatum*	gRNA construction
OJM673	R	ATGGTCTCTAAACACGCTTTGCATGGTGCGAACGACGAGCTTACTCGTTTCGTCCTCACGGACTCA	*P. digitatum*	gRNA construction
OJM678	F	GGTCGAAGCAAACACTCC	*P. digitatum*	RT construction. Amplification of 5' flank region of *wetA*. HR transformants screening
OJM679	R	CGATAGCGAATCCTAGCAGTCAAAGCAAAAGTACGGGGC	*P. digitatum*	RT construction. Amplification of 5' flank region of *wetA*.
OJM680	F	ACTGCTAGGATTCGCTATCGTTTTGATTCGATCCTCCA	*P. digitatum*	RT construction. Amplification of 3' flank region of *wetA*
OJM681	R	GATAGTGATGTAAAGACGG	*P. digitatum*	RT construction. Amplification of 3' flank region of *wetA*. HR transformants screening
OJM682	F	TCTAAACCACTGAACAGG	*P. digitatum*	RT construction. For 5' + 3' flank fusion of *wetA*
OJM683	R	CGGACTAAAGCAGCAAAGC	*P. digitatum*	RT construction. For 5' + 3' flank fusion of *wetA*
OJM684	F	GTTATTTGAGTTTTGGTCGC	*P. expansum*	RT construction. Amplification of 5' flank region of *wetA*. HR transformants screening
OJM685	R	CGATAGCGAATCCTAGCAGTTGGATGTGATTGGACAACC	*P. expansum*	RT construction. Amplification of 5' flank region of *wetA*
OJM686	F	ACTGCTAGGATTCGCTATCGTCTCTGTTTCTTTCAGCCG	*P. expansum*	RT construction. Amplification of 3' flank region of *wetA*
OJM687	R	AAAGGTAGGTCTTGCTGC	*P. expansum*	RT construction. Amplification of 3' flank region of *wetA*. HR transformants screening
OJM688	F	GCTTTATTTATTTGTGATGC	*P. expansum*	RT construction. For 5' + 3' flank fusion of *wetA*
OJM689	R	TAGATTGTTGAGATGTATGG	*P. expansum*	RT construction. For 5' + 3' flank fusion of *wetA*
OJM690	F	TTCTCTTTCACTCCAGACC	*P. digitatum*	Sanger sequencing
OJM691	R	CCCTCAATGCGGCTTCG	*P. digitatum*	Sanger sequencing
OJM692	F	TGTCTCCACTCCCAAACGCC	*P. expansum*	Sanger sequencing
OJM693	R	AGAGAGAGATGGTGAACGG	*P. expansum*	Sanger sequencing

705 **Table 1.** Oligonucleotides used in this study.

706 [a] F: forward; R: reverse.

707 [b] *Bsa*I restriction site is highlighted.

708 [c] gRNA: single guide RNA; RT: repair template; HR: Homologous recombination.

8. Figure captions

Fig. 1 Schematic representation of *P. digitatum* and *P. expansum* protoplast generation and transformation protocols

See main text for more details

Fig. 2 Application of CRISPR/Cas9 in *P. digitatum* to target *wetA*

A) Results of the transformation of *P. digitatum* with AMA1-based p15.0 plasmid through protoplast-mediated transformation for *wetA* disruption after 12 days of incubation at 25ºC. Arrows indicate the albino phenotype of the mutants. B) Molecular characterization of *P. digitatum* transformants with primers OJM678 and OJM681. Mutants showing white phenotypes are highlighted in red. Note that no HR occurred in any of the strains characterized. C) Nucleotide sequence alignment of Sanger sequencing results of *wetA* in the selected mutants. Protospacer for gRNA design is highlighted in red. Nucleotide alterations are highlighted in yellow. The PAM sequence is underlined

Fig. 3 Application of CRISPR/Cas9 in *P. expansum* to target *wetA*

A) Results of the transformation of *P. expansum* with AMA1-based p15.0 plasmid through protoplast-mediated transformation for *wetA* disruption after 7 days of incubation at 25 ºC. Arrow indicates the albino phenotype of a mutant. B) Molecular characterization of *P. expansum* transformants with primers OJM684 and OJM687. Mutants showing white phenotypes are highlighted in red. Note that the 2.6 kb band for Pe_16 shows HR. C) Nucleotide sequence alignment of Sanger sequencing results of *wetA* in the selected mutants. Protospacer for gRNA design is highlighted in red. Nucleotide alterations are highlighted in yellow. The PAM sequence is underlined

Fig. 4 Phenotypic characterization of Δ*wetA* mutants

A) Colony morphology of *P. digitatum* (left) and *P. expansum* (rigth) Δ*wetA* mutants on solid PDA plates after 8 days of growth. B) Growth on PDA plates determined by colony diameter measurement from 3 to 7 days of incubation. Data are mean values ± standard deviation (SD) of three technical replicates. C-D) Fruit infection assays of *P. digitatum* Δ*wetA* mutants on orange fruits. E-F) Fruit infection assays of *P.*

734 *expansum* Δ*wetA* mutants on apples. Data indicate the percentage of infected wounds (mean ± SD) at
735 each day post-inoculation (dpi). Asterisks (*) show statistical difference compared to the control at each
736 dpi (Student's *t*-test, $p<0.05$). D and F show representative images of orange and apple fruits,
737 respectively, infected by the indicated strains at 7 dpi

738 **Fig. 5 Conidia production and germination of Δ*wetA* mutants**

739 A) Conidia production per colony surface area of parental strains compared to Δ*wetA* mutants after 7
740 days of growth in PDA. B) Germination ability of Δ*wetA* mutants in 5% PDB represented as % of conidia,
741 germlings and germ tubes after 20 h of incubation for *P. digitatum* and 16 h for *P. expansum*. C)
742 Germination ability of Δ*wetA* mutants in H_2O represented as % of conidia, germlings and germ tubes after
743 72 h incubation at 25ºC. Data are mean values ± standard deviation (SD) of three technical replicates.
744 Asterisks (*) show significant differences between the mutant and the control strains (Student's *t*-test,
745 $p<0.05$).

746 **Fig. 6 Comparative antifungal activities of PeAfpA and PdAfpB against Δ*wetA* mutants**

747 Dose-response curves of growth inhibition of *P. expansum* Δ*wetA* mutants (A) and *P. digitatum* Δ*wetA*
748 mutants (B) by PeAfpA and PdAfpB. Curves show the mean ± standard deviation (SD) of triplicate
749 samples after 72 h of incubation at 25 °C

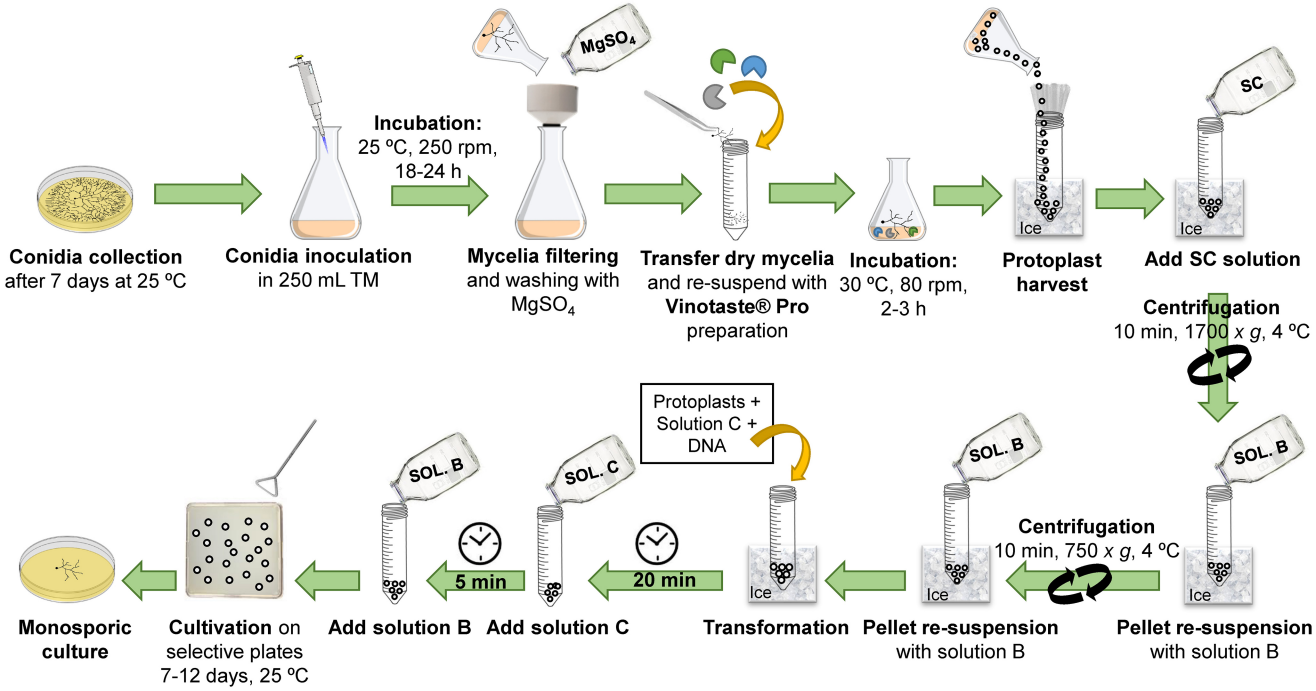
Conidia collection
after 7 days at 25 ºC
Conidia inoculation
in 250 mL TM
Incubation:
25 ºC, 250 rpm,
18-24 h
MgSO4
Mycelia filtering
and washing with
MgSO4
Transfer dry mycelia
and re-suspend with
Vinotaste® Pro
preparation
Incubation:
30 ºC, 80 rpm,
2-3 h
Ice
Protoplast
harvest
SC
Ice
Add SC solution
Centrifugation
10 min, 1700 x g, 4 ºC
SOL. B
Ice
Pellet re-suspension
with solution B
Centrifugation
10 min, 750 x g, 4 ºC
SOL. B
Ice
Pellet re-suspension
with solution B
Protoplasts +
Solution C +
DNA
Ice
Transformation
SOL. C
20 min
Add solution C
SOL. B
5 min
Add solution B
Cultivation on
selective plates
7-12 days, 25 ºC
Monosporic
culture

A

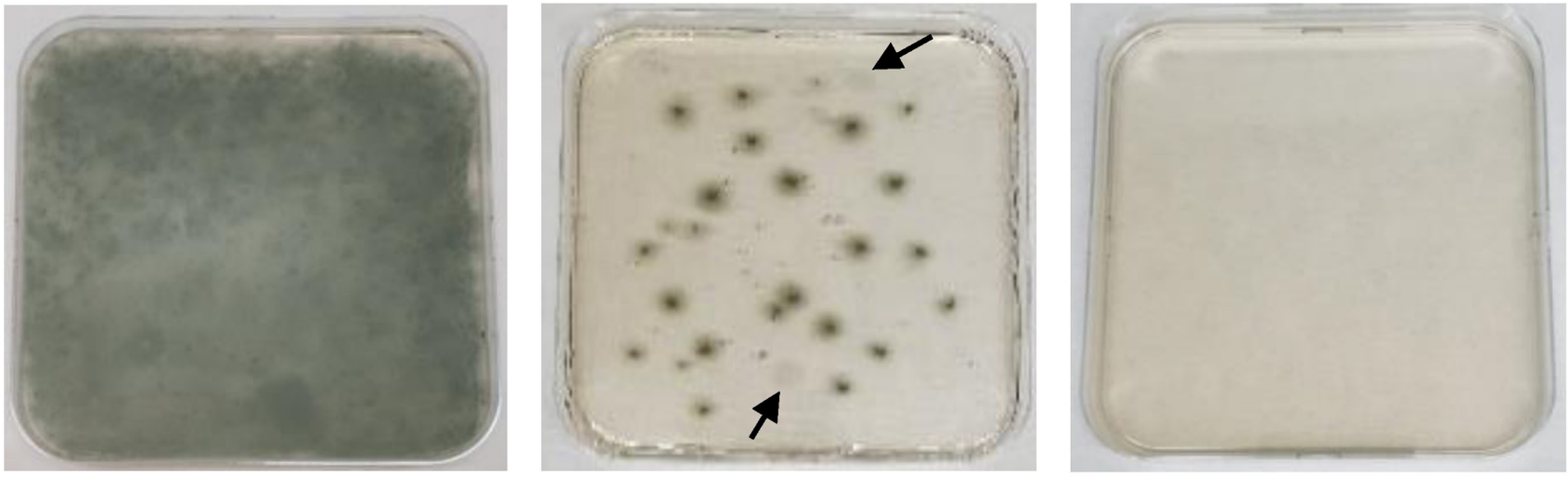

Regeneration control | Transformation | Negative control

B

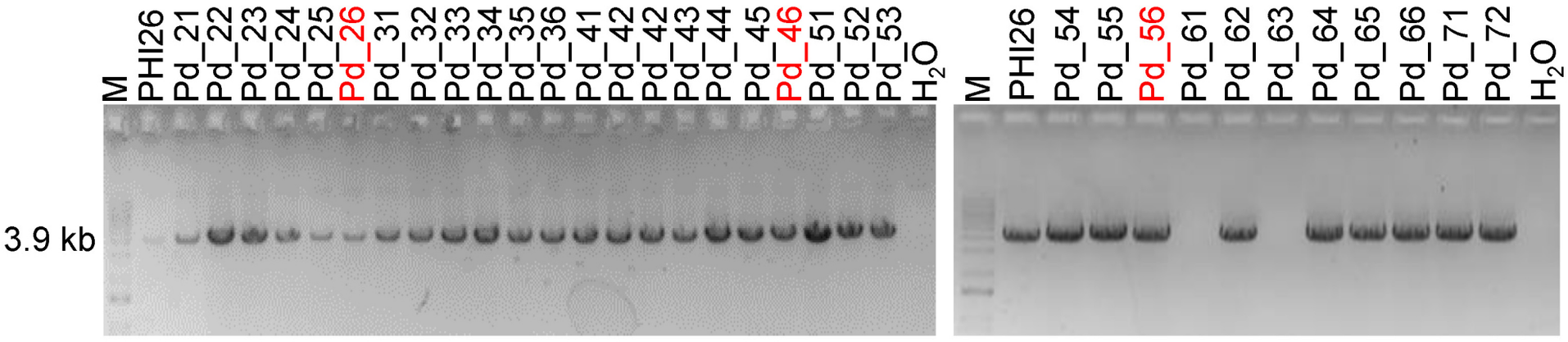

C

```
Pd_wetA_ref   ATGGTGGTCCCCCATGACTTCTCGGGTCGCTCAACAACAGGCCTCTTACCTCACGTCTCC   60
Pd_46         ATGGTGGTCCCCCATGACTTCTCGGGTCGCTCAACAACAGGCCTCTTACCTCACGTCTCC   60
Pd_26         ATGGTGGT-CCCCATGACTTCTCGGGTCGCTCAACAACAGGCCTCTTACCTCACGTCTCC   59
Pd_56         ATGGTGGTCCCCCATGACTTCTCGGGTCGCTCAACAACAGGCCTCTTACCTCACGTCTCC   60
              ******** ******************************************************

Pd_wetA_ref   CACGCCTGTTCGCACCATGCAAAGCGTTGGAAGCCAAAATGACATTATGCAAGGAGGACT   120
Pd_46         CACGCCTGTTCGCACCATGCAAAG-GTTGGAAGCCAAAATGACATTATGCAAGGAGGACT   119
Pd_26         CACGCCTGTTCGCACCATGCAAAGCGTTGGAAGCCAAAATGACATTATGCAAGGAGGACT   119
Pd_56         CACGCCTGTTCGCACCATGCAA-GCGTTGGAAGCCAAAATGACATTATGCAAGGAGGACT   119
              ********************** * ***********************************
```

A

B

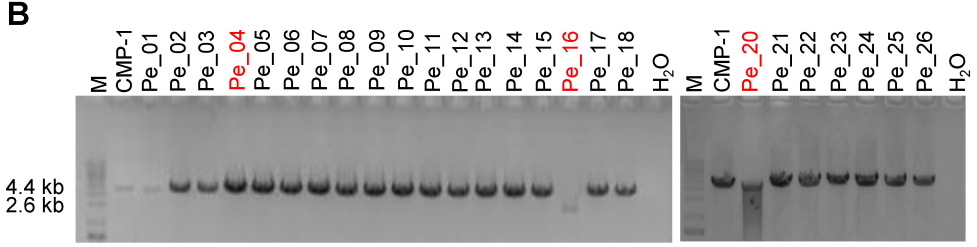

C

```
Pe_wetA_ref    CAATCCTTCCTACGACATGTCGGCGGAACACCCATTCTCATCATCTAATATGCTCCCCGC   120
Pe_04          CAATCCTTCCTACGACA-GTCGGCGGAACACCCATTCTCATCATCTAATATGCTCCCCGC   119
Pe_20          CAATCCTTCCTACGACATG-CGGCGGAACACCCATTCTCATCATCTAATATGCTCCCCGC   119
               **************** * ************************************

Pe_wetA_ref    CACCTCTCAAAAATTCGACA        140
Pe_04          CACCTCTCAAAAAT-CGACA        138
Pe_20          CACCTCTCAAAAATTCGACA        139
               ************** *****
```

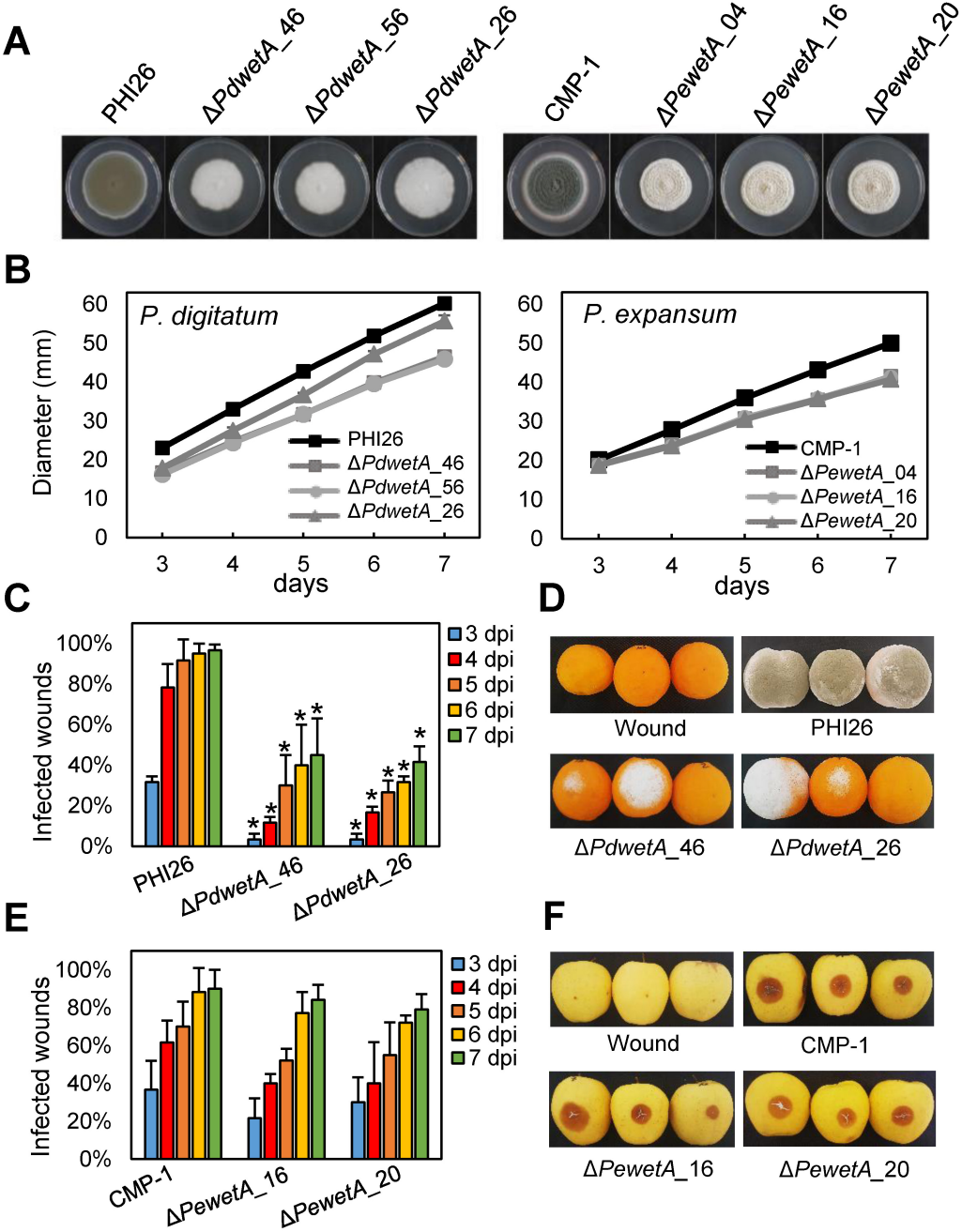
A
PHI26
ΔPdwetA_46
ΔPdwetA_56
ΔPdwetA_26
CMP-1
ΔPewetA_04
ΔPewetA_16
ΔPewetA_20
B
P. digitatum
Diameter (mm)
days
PHI26
ΔPdwetA_46
ΔPdwetA_56
ΔPdwetA_26
P. expansum
CMP-1
ΔPewetA_04
ΔPewetA_16
ΔPewetA_20
C
Infected wounds
3 dpi
4 dpi
5 dpi
6 dpi
7 dpi
PHI26
ΔPdwetA_46
ΔPdwetA_26
D
Wound
PHI26
ΔPdwetA_46
ΔPdwetA_26
E
Infected wounds
CMP-1
ΔPewetA_16
ΔPewetA_20
F
Wound
CMP-1
ΔPewetA_16
ΔPewetA_20

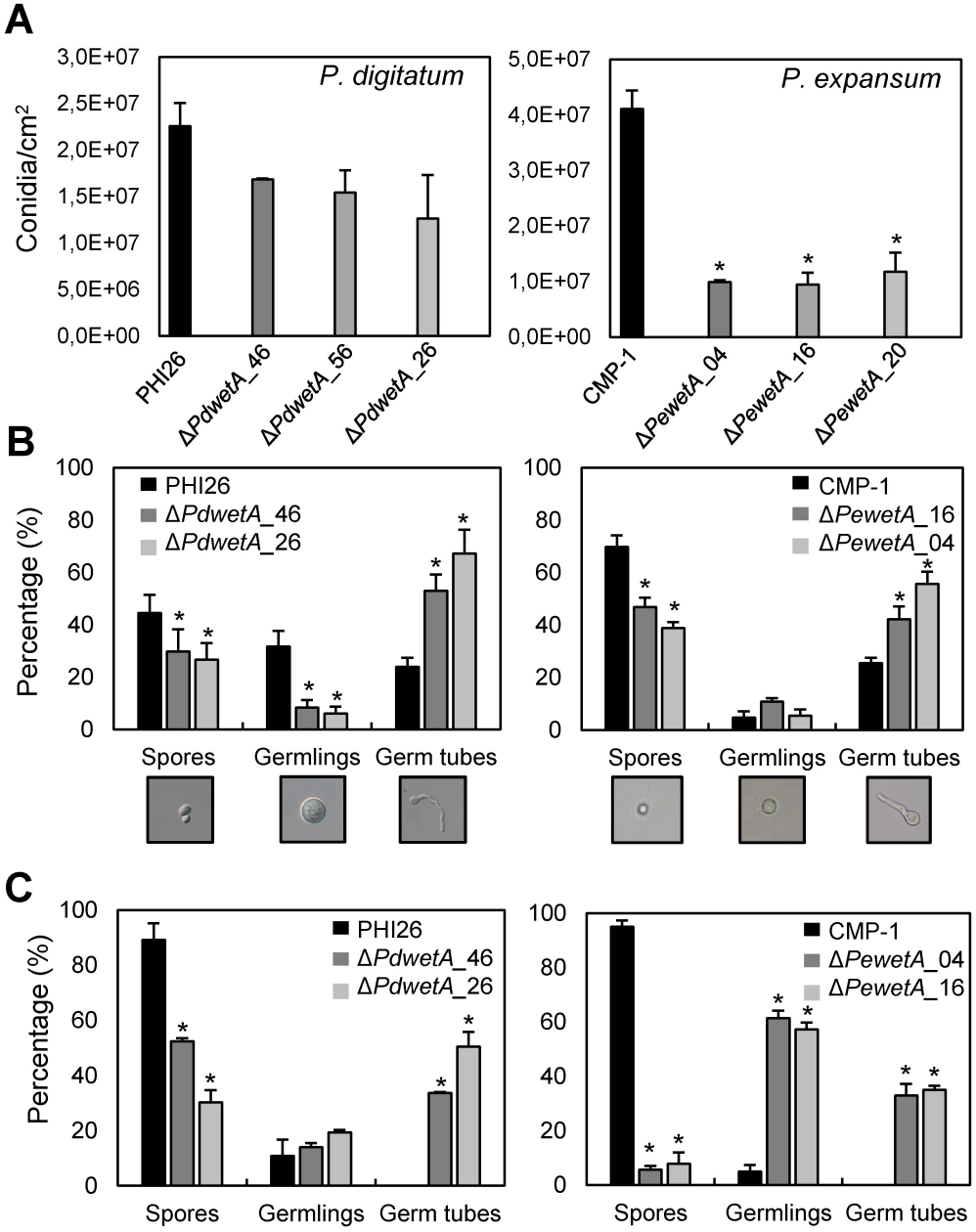
A
Conidia/cm2
P. digitatum
3,0E+07
2,5E+07
2,0E+07
1,5E+07
1,0E+07
5,0E+06
0,0E+00
PHI26
ΔPdwetA_46
ΔPdwetA_56
ΔPdwetA_26
P. expansum
5,0E+07
4,0E+07
3,0E+07
2,0E+07
1,0E+07
0,0E+00
CMP-1
ΔPewetA_04
ΔPewetA_16
ΔPewetA_20
B
Percentage (%)
PHI26
ΔPdwetA_46
ΔPdwetA_26
CMP-1
ΔPewetA_16
ΔPewetA_04
Spores
Germlings
Germ tubes
C
Percentage (%)
PHI26
ΔPdwetA_46
ΔPdwetA_26
CMP-1
ΔPewetA_04
ΔPewetA_16
Spores
Germlings
Germ tubes

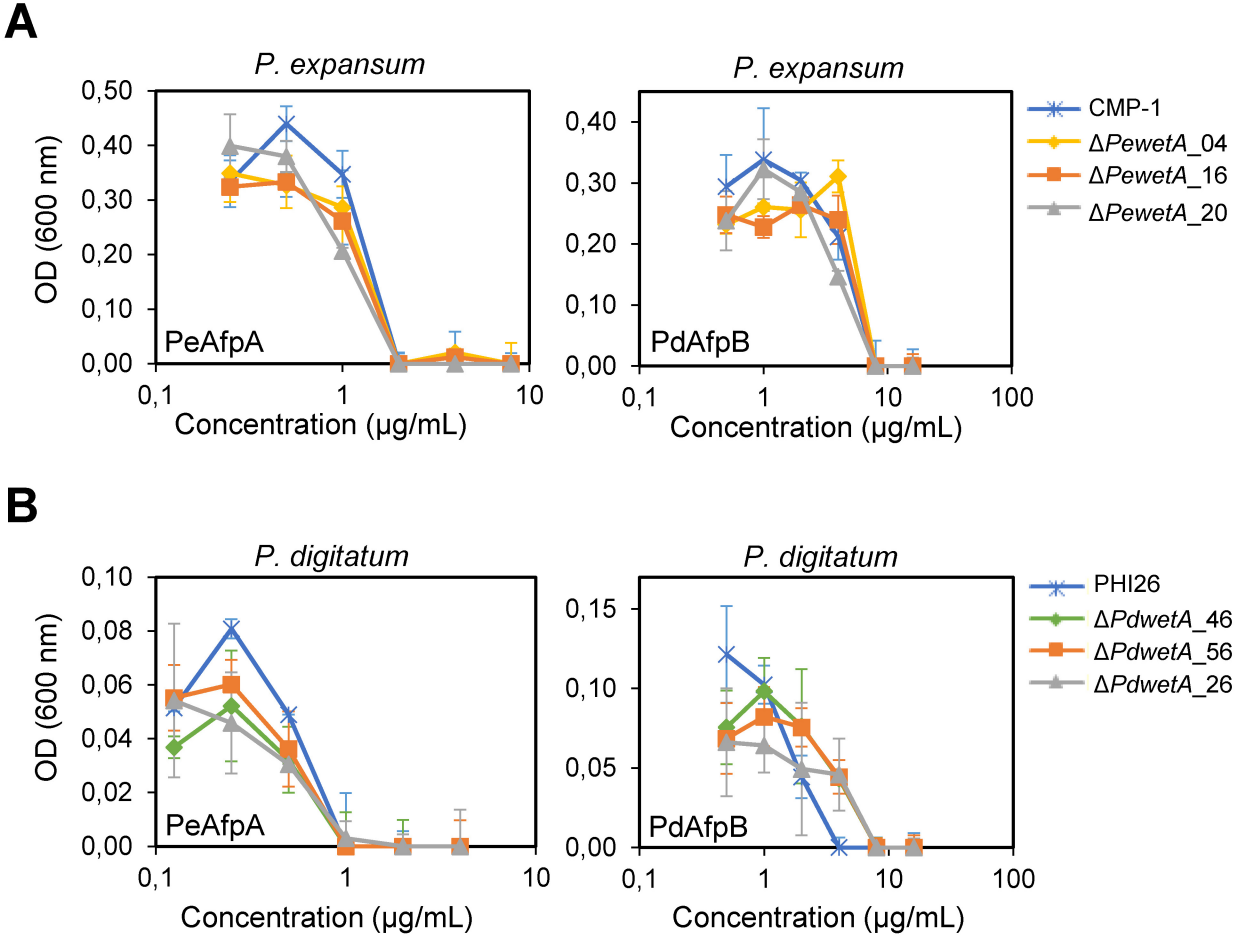
A
P. expansum
OD (600 nm)
0,50
0,40
0,30
0,20
0,10
0,00
PeAfpA
0,1
1
10
Concentration (µg/mL)
P. expansum
0,40
0,30
0,20
0,10
0,00
PdAfpB
0,1
1
10
100
Concentration (µg/mL)
CMP-1
ΔPewetA_04
ΔPewetA_16
ΔPewetA_20
B
P. digitatum
OD (600 nm)
0,10
0,08
0,06
0,04
0,02
0,00
PeAfpA
0,1
1
10
Concentration (µg/mL)
P. digitatum
0,15
0,10
0,05
0,00
PdAfpB
0,1
1
10
100
Concentration (µg/mL)
PHI26
ΔPdwetA_46
ΔPdwetA_56
ΔPdwetA_26